Reduced order finite element formulations for vibration reduction using piezoelectric shunt damping

Walid Larbi, Jean-François Deü

Version of Record: https://www.sciencedirect.com/science/article/pii/S0003682X17307028
Manuscript_f7850a74f6a8d83bebe55d3ae084043c

Reduced order finite element formulations for vibration reduction using piezoelectric shunt damping

W. Larbi*, J.-F. Deü

Structural Mechanics and Coupled Systems Laboratory,
Conservatoire National des Arts et Métiers,
292 rue Saint-Martin, 75141 Paris Cedex 03, France

Abstract

The present work proposes an original reduced order models for prediction of passive reduction of structural vibration by means of shunted piezoelectric patches. The problem consists of an elastic structure with surface-mounted piezoelectric patches. The piezoelectric elements are connected to a resonant shunt circuits in order to damp specific resonant frequencies of the structure. An efficient electromechanical finite element formulation for the dynamic analysis of the problem is first presented. The classical modal superposition techniques using the system eigenvectors with all patches short-circuited or open-circuited are then recalled. An advanced reduced order models using two new modal projection bases able to solve the problem at lower cost are developed: (i) the combined basis formed by both the short-circuited and open-circuited modes, and (ii) the coupled basis formed by the electromechanical modes that take into account the effect of the inductances of the electrical shunt circuits. Various numerical and experimental results are presented in order to validate and illustrate the efficiency of the proposed new finite element reduced order formulations.

Keywords: Vibration reduction; Piezoelectric patches; Shunt damping; Modal superposition; Reduced order model.

*Corresponding author. Email: walid.larbi@cnam.fr Tel. 0033140272793 Fax 0033140272502

1. Introduction

Piezoelectric materials are widely used in vibration damping and noise reduction. These materials, which enable the transformation of mechanical energy into electrical energy (direct piezoelectric effect) and vice-versa (inverse piezoelectric effect), allow direct connection with an input/output electrical signal and make them well adapted to distributed sensing and actuation. This work is focused on passive control strategies using piezoelectric elements for vibration damping. As compared to the active control techniques, passive techniques have the advantage of being simple to implement, always stable and do not require digital signal processors and bulky power amplifiers. Examples of active control systems can be found for example in [1, 2].

In this paper, the specific application of passive vibration reduction by means of shunted piezoelectric patches is addressed. In this technology, the elastic structure is equipped with piezoelectric patches that are connected to a passive electrical circuit, called a shunt. The piezoelectric patches transform mechanical energy of the vibrating structure into electrical energy, which is then dissipated into the form of Joule heat to provide electrical damping to the structure by the shunt circuits. Several shunt circuits can be considered: the classical R- and RL-shunts, proposed by Hagood and Von Flotow [3], improvements of those techniques, by the use of several piezoelectric elements [4, 5, 6], active fiber composites [7] or adaptive shunts [8], and recently semi-passive techniques, commonly known as "switch" techniques [9, 10, 11]. Since those techniques are passive (or semi-passive if some electronic components have to be powered), a critical issue is that their performances, in terms of damping efficiency, directly depend on the electromechanical coupling between the host structure and the piezoelectric elements, which has to be maximized.

The present work concerns the numerical modeling of vibration reduction of elastic structures in the low frequency range by using shunted piezoelectric elements. The aim is to propose efficient reduced order finite element models able to predict the shunt damping. An electromechanical finite element formulation for the dynamic analysis of smart structures with piezoelectric elements is first proposed. In this formulation, the electrical state is fully described by very few global discrete unknowns [12]: (i) the electric charge contained in the electrodes and (ii) the voltage between the electrodes. This formulation is well adapted to practical applications since realistic electrical

boundary conditions, such that equipotentiality on the electrodes and prescribed global electric charges, naturally appear. The charge/voltage global variables are also intrinsically adapted to include any external electrical circuit into the electromechanical problem and to simulate the effect of shunt damping techniques. We present then different strategies to solve the problem using a modal reduction approach. In this technique, the electromechanical coupled system is solved by projecting the mechanical displacement unknown on a truncated basis composed by the first structural normal modes while the few initial electrical unknowns are kept in the reduced system. The projection bases widely used in the literature are obtained using the short-circuited or open-circuited eigenvalue problems [13, 14]. The originality of this paper lies in proposing a new reduced order models using two new modal projection bases able to solve the problem at lower cost: (i) the combined basis formed by both the short-circuited and open-circuited modes, and (ii) the coupled basis formed by the electromechanical modes that take into account the effect of the inductances of the electrical shunts circuit. Numerical examples are finally presented in order to evaluate the effectiveness of the proposed new strategies of modal projection compared to the classic ones in terms of prediction of the vibration attenuation using piezoelectric shunt systems.

2. Finite element formulation

We briefly recall in this section the finite element formulation of an elastic structure with surface mounted shunted piezoelectric patches.

An elastic structure occupying the domain Ω_E is equipped with P piezoelectric patches (figure 1). Each piezoelectric patch is covered on its upper and lower surfaces with a very thin electrode. The pth patch, $p \in \{1, \cdots, P\}$, occupies a domain $\Omega^{(p)}$ such that $(\Omega_E, \Omega^{(1)}, \cdots, \Omega^{(P)})$ is a partition of the all structure domain Ω_S. In order to reduce the vibration amplitudes of the problem, a resonant shunt circuit made up of a resistance $R^{(p)}$ and an inductance $L^{(p)}$ in series is connected to each patch [3, 11].

Moreover, the structure is clamped on a part Γ_u and subjected to a given surface force density F_i^d on the complementary part Γ_σ of its external boundary.

For each piezoelectric patch, a set of hypotheses, which can be applied to a wide spectrum of practical applications, are formulated:

- The piezoelectric patches are thin, with a constant thickness, denoted $h^{(p)}$ for the pth patch;

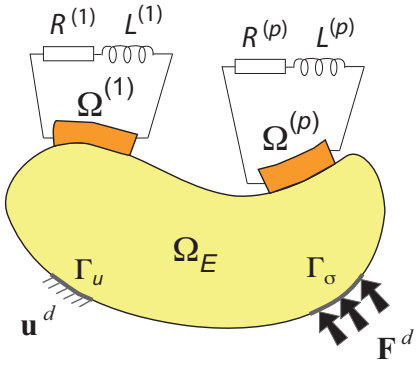

Figure 1: Vibrating structure connected to RL shunt circuits.

- The thickness of the electrodes is much smaller than $h^{(p)}$ and is thus neglected;
- The piezoelectric patches are polarized in their transverse direction (i.e. the direction normal to the electrodes).

Under those assumptions, the electric field vector, of components $E_k^{(p)}$, can be considered normal to the electrodes and uniform in the piezoelectric patch [12], so that for all $p \in \{1, \cdots, P\}$:

$$E_k^{(p)} = -\frac{V^{(p)}}{h^{(p)}} n_k \quad \text{in} \quad \Omega^{(p)} \tag{1}$$

where E_i is the electric field, $V^{(p)}$ is the potential difference between the upper and the lower electrode surfaces of the pth patch which is constant over $\Omega^{(p)}$ and n_k is the kth component of the normal unit vector to the surface of the electrodes.

After variational formulation and finite element discretization, we obtain the following matrix system in frequency domain:

$$\begin{bmatrix} \mathbf{K}_u & \mathbf{C}_{uV} \\ -\mathbf{C}_{uV}^T & \mathbf{K}_V \end{bmatrix} \begin{bmatrix} \mathbf{U} \\ \mathbf{V} \end{bmatrix} - \omega^2 \begin{bmatrix} \mathbf{M}_u & \mathbf{0} \\ \mathbf{0} & \mathbf{0} \end{bmatrix} \begin{bmatrix} \mathbf{U} \\ \mathbf{V} \end{bmatrix} = \begin{bmatrix} \mathbf{F} \\ \mathbf{Q} \end{bmatrix} \tag{2}$$

where $\mathbf{U}$ is the column vector of nodal values of mechanical displacement of length N_s (N_s is the number of mechanical degrees of freedom); $\mathbf{M}_u$ and $\mathbf{K}_u$ are the mass and stiffness matrices of the structure (elastic structure and piezoelectric patches) of size $N_s \times N_s$ and $\mathbf{F}$ is the applied mechanical

force vector of length N_s. Note that $\mathbf{F}$ is composed of two parts: $\mathbf{F}_0$ is the invariant spatial portion and $f(\omega)$ is the frequency varying portion. With this decomposition $\mathbf{F}$ can be written as $\mathbf{F} = \mathbf{F}_0 f(\omega)$.

Moreover, $\mathbf{Q} = (Q^{(1)}\, Q^{(2)} \cdots Q^{(P)})^T$ and $\mathbf{V} = (V^{(1)}\, V^{(2)} \cdots V^{(P)})^T$ are the column vectors of electric charges and potential differences; $\mathbf{C}_{uV}$ is the electric mechanical coupled stiffness matrix of size $N_s \times P$; $\mathbf{K}_V = \text{diag}\left(C^{(1)}\, C^{(2)} \cdots C^{(P)}\right)$ is a diagonal matrix filled with the P capacitances of the piezoelectric patches where $C^{(p)} = \epsilon_{33} S^{(p)}/h^{(p)}$, ϵ_{33} being the piezoelectric permittivity in the direction normal to the electrodes and $S^{(p)}$ the area of the patch electrodes surfaces.

The above discretized equation is adapted to any elastic structure with surface-mounted piezoelectric patches. Its originality lies in the fact that the system electrical state is fully described by very few global discrete unknowns: only a couple of variables per piezoelectric patch, namely (1) the electric charge contained in the electrodes and (2) the voltage between the electrodes. Once the electrical part of the problem is fully discretized at the weak formulation step, by introducing the above cited voltage/charge variables, without any restriction on the mechanical part of the problem, any standard FE formulation can be easily modified to include the piezoelectric patches and thus the effect of an external electrical action. A second advantage of this formulation is that since global electrical variables are used, realistic electrical boundary conditions are naturally introduced. First, the equipotentiality in any of the patches electrodes is exactly satisfied when introducing the potential difference variable. Second, the use of the global charge contained in the electrodes, as the second electrical variable, is realistic since plugging an external electrical circuit to the electrodes of the patches imposes only the global charge contained in the electrodes and not a local charge surface density. Another advantage of using the global charge voltage variables is that they are intrinsically adapted to include any external electrical circuit into the electromechanical problem and to simulate the effect of shunt damping techniques. In this case, neither $\mathbf{V}$ nor $\mathbf{Q}$ is prescribed by the electrical network but the latter imposes only a relation between them [3]. For the case of a resonant shunt composed of a resistor R and an inductor L in series, connected to the pth patch, the relation writes

$$-\omega^2 L^{(p)} Q^{(p)} + i\omega R^{(p)} Q^{(p)} + V^{(p)} = 0 \tag{3}$$

Combining Eqs. (2) and (3), we finally obtain the general FE formulation of the electromechanical spectral problem when the piezoelectric patches are

shunted

$$-\omega^2 \begin{bmatrix} \mathbf{M}_u & \mathbf{0} \\ \mathbf{0} & \mathbf{L} \end{bmatrix} \begin{bmatrix} \mathbf{U} \\ \mathbf{Q} \end{bmatrix} + i\omega \begin{bmatrix} \mathbf{0} & \mathbf{0} \\ \mathbf{0} & \mathbf{R} \end{bmatrix} \begin{bmatrix} \mathbf{U} \\ \mathbf{Q} \end{bmatrix} + \begin{bmatrix} \mathbf{K}_u + \mathbf{C}_{uV}\mathbf{K}_V^{-1}\mathbf{C}_{uV}^T & \mathbf{C}_{uV}\mathbf{K}_V^{-1} \\ \mathbf{K}_V^{-1}\mathbf{C}_{uV}^T & \mathbf{K}_V^{-1} \end{bmatrix} \begin{bmatrix} \mathbf{U} \\ \mathbf{Q} \end{bmatrix} = \begin{bmatrix} \mathbf{F} \\ \mathbf{0} \end{bmatrix} \quad (4)$$

where $\mathbf{R} = \text{diag}\left(R^{(1)}\, R^{(2)} \cdots R^{(P)}\right)$ and $\mathbf{L} = \text{diag}\left(L^{(1)}\, L^{(2)} \cdots L^{(P)}\right)$ are the diagonal matrices filled with the electrical resistances and the electrical inductances of the shunt circuits. Note that since $\mathbf{K}_V$ is diagonal, the evaluation of $\mathbf{K}_V^{-1}$ is straightforward.

3. Reduced order models

In order to evaluate the electromechanical frequency response functions of an elastic structure with shunted piezoelectric patches and subjected to a harmonic mechanical excitation, the full finite element model of Eq. (4) is applicable only to a small model and low frequency band. To overcome these limitations, a model reduction approach based on a normal mode expansion and truncation of high-frequency modes is proposed in this section. We present first a review of the existing reduced order models. The models, widely used in the literature, are obtained using the short-circuited or open-circuited bases. We propose then two original reduced order models using two new modal projection bases and able to solve the problem at lower cost: (i) the combined basis formed by both the short-circuited and open-circuited modes, and (ii) the coupled basis formed by the electromechanical modes taking into account the effect of the inductances of the electrical shunt circuits. A comparative study on the effectiveness of theses reduced-order models in terms of prediction vibration damping using piezoelectric shunt systems is proposed in next section.

3.1. Projection on the short-circuited basis

The first M_s eigenmodes of the elastic structure with all patches short-circuited are obtained from the following equation:

$$\left[\mathbf{K}_u - \omega_i^2 \mathbf{M}_u\right] \mathbf{\Phi}_i = \mathbf{0} \quad \text{for } i \in \{1, \cdots, M_s\} \quad (5)$$

where $(\omega_i, \mathbf{\Phi}_i)$ are the natural frequency and eigenvector for the ith structural mode. These modes verify the following orthogonality properties

$$\mathbf{\Phi}_i^T \mathbf{M}_u \mathbf{\Phi}_j = \delta_{ij} \quad \text{and} \quad \mathbf{\Phi}_i^T \mathbf{K}_u \mathbf{\Phi}_j = \omega_i^2 \delta_{ij} \quad (6)$$

where δ_{ij} is the Kronecker symbol and $\mathbf{\Phi}_i$ have been normalized with respect to the structure mass matrix. Note that the structure is fixed on Γ_u, which eliminates any rigid body motion.

By introducing the modal matrix $\mathbf{\Phi} = [\mathbf{\Phi}_1 \cdots \mathbf{\Phi}_{M_s}]$ of size $(N_s \times M_s)$, N_s is the total number of degrees of freedom in the finite elements model associated to the structure, the displacement $\mathbf{U}$ is sought as

$$\mathbf{U} = \mathbf{\Phi}\mathbf{q}(\omega) \tag{7}$$

where the vector $\mathbf{q} = [q_1 \cdots q_{M_s}]^T$ is the unknown modal amplitudes.

By applying the Ritz-Galerkin projection method, which consists of substituting Eq. (7) into Eq. (4) and premultiplying the first row by $\mathbf{\Phi}^T$, we obtain the reduced matrix system

$$\begin{aligned} &-\omega^2 \begin{bmatrix} \mathbf{\Phi}^T\mathbf{M}_u\mathbf{\Phi} & \mathbf{0} \\ \mathbf{0} & \mathbf{L} \end{bmatrix} \begin{bmatrix} \mathbf{q} \\ \mathbf{Q} \end{bmatrix} + i\omega \begin{bmatrix} \mathbf{0} & \mathbf{0} \\ \mathbf{0} & \mathbf{R} \end{bmatrix} \begin{bmatrix} \mathbf{q} \\ \mathbf{Q} \end{bmatrix} + \\ &\begin{bmatrix} \mathbf{\Phi}^T\left(\mathbf{K}_u + \mathbf{C}_{uV}\mathbf{K}_V^{-1}\mathbf{C}_{uV}^T\right)\mathbf{\Phi} & \mathbf{\Phi}^T\mathbf{C}_{uV}\mathbf{K}_V^{-1} \\ \mathbf{K}_V^{-1}\mathbf{C}_{uV}^T\mathbf{\Phi} & \mathbf{K}_V^{-1} \end{bmatrix} \begin{bmatrix} \mathbf{q} \\ \mathbf{Q} \end{bmatrix} = \begin{bmatrix} \mathbf{\Phi}_s^T\mathbf{F} \\ \mathbf{0} \end{bmatrix} \end{aligned} \tag{8}$$

This matrix equation represents the reduced-order model using the short-circuited basis of the vibration reduction problem with piezoelectric shunt-damping treatments. If only few modes are kept for the projection, the size of this reduced-order model $(Ms + P)$ is much smaller than the initial one $(Ns + P)$. Eq. (8) can be also written in the following form of coupled differential equations:

- M_s mechanical oscillators

$$-\omega^2 q_i + 2i\omega\xi_i\omega_i q_i + \omega_i^2 q_i + \sum_{p=1}^{P}\sum_{k=1}^{N_s} \frac{\gamma_i^{(p)}\gamma_k^{(p)}}{C^{(p)}} q_i + \sum_{p=1}^{P} \frac{\gamma_i^{(p)}}{C^{(p)}} Q^{(p)} = F_i \tag{9}$$

- P electrical equations

$$-\omega^2 L^{(p)}Q^{(p)} + i\omega R^{(p)}Q^{(p)} + \frac{Q^{(p)}}{C^{(p)}} + \sum_{i=1}^{N_s} \frac{\gamma_i}{C^{(p)}} q_{si} = 0 \tag{10}$$

where $F_i = \mathbf{\Phi}_i^T\mathbf{F}$ is the mechanical excitation of the ith mode and $\gamma_i = \mathbf{\Phi}_i^T\mathbf{C}_{uV}$ is the electromechanical coupling factor.

Note that the modal damping coefficients ξ_i have been added in Eq. (9) in order to take into account the structural damping, which can be measured experimentally. This is mandatory in order to quantify the attenuation due to the shunt at the resonance (of course, without damping, the amplitude of the response at the resonance is theoretically infinite).

The major interest of choosing the short-circuit eigenmodes as the expansion basis is that its can be computed with a classical elastic mechanical problem. This operation can thus be done by any standard finite elements code.

3.2. Projection on the open-circuited basis

The first M_s natural frequencies $\widehat{\omega}_i$ and eigenvectors $\widehat{\mathbf{\Phi}}_i$ of the elastic structure with all patches open-circuited are obtained from the following equation:

$$\left[(\mathbf{K}_u + \mathbf{C}_{uV}\mathbf{K}_V^{-1}\mathbf{C}_{uV}^T) - \widehat{\omega}_i^2\mathbf{M}_u\right]\widehat{\mathbf{\Phi}}_i = \mathbf{0} \quad \text{for } i \in \{1, \cdots, M_s\} \tag{11}$$

These modes verify the following orthogonality properties

$$\widehat{\mathbf{\Phi}}_i^T\mathbf{M}_u\widehat{\mathbf{\Phi}}_j = \delta_{ij} \quad \text{and} \quad \widehat{\mathbf{\Phi}}_i^T(\mathbf{K}_u + \mathbf{C}_{uV}\mathbf{K}_V^{-1}\mathbf{C}_{uV}^T)\widehat{\mathbf{\Phi}}_j = \widehat{\omega}_i^2\delta_{ij} \tag{12}$$

Thus, the displacement $\mathbf{U}$ is sought as

$$\mathbf{U} = \widehat{\mathbf{\Phi}}\widehat{\mathbf{q}}(t) \tag{13}$$

where the matrix $\widehat{\mathbf{\Phi}} = \left[\widehat{\mathbf{\Phi}}_1 \cdots \widehat{\mathbf{\Phi}}_{M_s}\right]$ of size $(N_s \times M_s)$ corresponds to the projection basis constituted by the first M_s eigenmodes of the structure with all patches open-circuited and where the vector $\widehat{\mathbf{q}} = [\widehat{q}_1 \cdots \widehat{q}_{M_s}]^T$ is the unknown modal amplitudes.

By applying the Ritz-Galerkin projection method using the procedure described in section 3.1, we obtain the following coupled differential equations:

- M_s mechanical oscillators

$$-\omega^2\widehat{q}_i + 2i\omega\xi_i\widehat{\omega}_i\widehat{q}_i + {\widehat{\omega}_i}^2\widehat{q}_i + \sum_{p=1}^{P}\frac{\widehat{\gamma}_i^{(p)}}{C^{(p)}}Q^{(p)} = \widehat{F}_i \tag{14}$$

- P electrical equations

$$-\omega^2 L^{(p)} Q^{(p)} + i\omega R^{(p)} Q^{(p)} + \frac{Q^{(p)}}{C^{(p)}} + \sum_{i=1}^{N_s} \frac{\widehat{\gamma}_i}{C^{(p)}} \widehat{q}_i = 0 \tag{15}$$

where $\widehat{F}_i = \widehat{\mathbf{\Phi}}_i^T \mathbf{F}$ and $\widehat{\gamma}_i = \widehat{\mathbf{\Phi}}_i^T \mathbf{C}_{uV}$ are the mechanical excitation and the electromechanical coupling factor of the ith mode respectively.

3.3. Projection on the combined basis

This method consists in building a projection basis formed by both the short-circuited and open-circuited modes:

$$\mathbf{\Phi}_c = \left[\mathbf{\Phi} \; \widehat{\mathbf{\Phi}} \right] = \left[\mathbf{\Phi}_1 \cdots \mathbf{\Phi}_{M_s} \, \widehat{\mathbf{\Phi}}_1 \cdots \widehat{\mathbf{\Phi}}_{M_s} \right] \tag{16}$$

Thus, the displacement $\mathbf{U}$ is sought as

$$\mathbf{U} = \mathbf{\Phi}_c \mathbf{q}_c(t) = \mathbf{\Phi} \mathbf{q}(t) + \widehat{\mathbf{\Phi}} \widehat{\mathbf{q}}(t) \tag{17}$$

By applying the Ritz-Galerkin projection method, which consists of substituting Eq. (17) into Eq. (4) and premultiplying the first row by $\mathbf{\Phi}_c^T$, we obtain the reduced matrix system,

$$\begin{aligned} &-\omega^2 \begin{bmatrix} \mathbf{\Phi}_c^T \mathbf{M}_u \mathbf{\Phi}_c & \mathbf{0} \\ \mathbf{0} & \mathbf{L} \end{bmatrix} \begin{bmatrix} \mathbf{q}_c \\ \mathbf{Q} \end{bmatrix} + i\omega \begin{bmatrix} \mathbf{0} & \mathbf{0} \\ \mathbf{0} & \mathbf{R} \end{bmatrix} \begin{bmatrix} \mathbf{q}_c \\ \mathbf{Q} \end{bmatrix} + \\ &\begin{bmatrix} \mathbf{\Phi}_c^T \left(\mathbf{K}_u + \mathbf{C}_{uV} \mathbf{K}_V^{-1} \mathbf{C}_{uV}^T \right) \mathbf{\Phi}_c & \mathbf{\Phi}_c^T \mathbf{C}_{uV} \mathbf{K}_V^{-1} \\ \mathbf{K}_V^{-1} \mathbf{C}_{uV}^T \mathbf{\Phi}_c & \mathbf{K}_V^{-1} \end{bmatrix} \begin{bmatrix} \mathbf{q}_c \\ \mathbf{Q} \end{bmatrix} = \begin{bmatrix} \mathbf{\Phi}_c^T \mathbf{F} \\ \mathbf{0} \end{bmatrix} \end{aligned} \tag{18}$$

For this technique, two drawbacks exist: (i) two modal analysis are required and (ii) the short-circuited and open-circuited eigenvectors are not mutually orthogonal with respect to the mass and stiffness matrices of the problem. Thus, a Gram-Schmidt algorithm is applied in this work to orthogonalize these eigenvectors and build well-conditioned matrices.

3.4. Projection on the coupled basis

In the case of a resonant shunt, this technique consists in computing the eigenmodes of the real conservative system associated to Eq. (4). Thus, the inductances of the shunt circuits are taken into account in the mass matrix,

whereas the effect of the resistances and mechanical damping is not considered. The eigenmode $(\tilde{\omega}_i, \tilde{\mathbf{\Phi}}_i)$ of this problem is solution of the following equation:

$$\left(-\tilde{\omega}_i^2 \begin{bmatrix} \mathbf{M}_u & \mathbf{0} \\ \mathbf{0} & \mathbf{L} \end{bmatrix} + \begin{bmatrix} \mathbf{K}_u + \mathbf{C}_{uV}\mathbf{K}_V^{-1}\mathbf{C}_{uV}^T & \mathbf{C}_{uV}\mathbf{K}_V^{-1} \\ \mathbf{K}_V^{-1}\mathbf{C}_{uV}^T & \mathbf{K}_V^{-1} \end{bmatrix}\right) \tilde{\mathbf{\Phi}}_i = \begin{bmatrix} \mathbf{0} \\ \mathbf{0} \end{bmatrix} \quad (19)$$

where the eigenvector $\tilde{\mathbf{\Phi}}_i^T = \begin{bmatrix} \tilde{\mathbf{\Phi}}_{si}^T & \tilde{\mathbf{\Phi}}_{qi}^T \end{bmatrix}$ consists of the mechanical degrees-of-freedom $\tilde{\mathbf{\Phi}}_{si}$ of size N_s followed by the electric degrees-of-freedom $\tilde{\mathbf{\Phi}}_{qi}$ of size P.

By introducing the modal basis $\tilde{\mathbf{\Phi}} = \left[\tilde{\mathbf{\Phi}}_{s1} \cdots \tilde{\mathbf{\Phi}}_{sM_s}\right]$ of size $(N_s \times M_s)$, the displacement $\mathbf{U}$ is sought as

$$\mathbf{U} = \tilde{\mathbf{\Phi}}\tilde{\mathbf{q}}(t) \quad (20)$$

By applying the Ritz-Galerkin projection method, which consists of substituting Eq. (20) into Eq. (4) and premultiplying the first row by $\tilde{\mathbf{\Phi}}^T$, we obtain the reduced matrix system,

$$\begin{aligned} &-\omega^2 \begin{bmatrix} \tilde{\mathbf{\Phi}}^T\mathbf{M}_u\tilde{\mathbf{\Phi}} & \mathbf{0} \\ \mathbf{0} & \mathbf{L} \end{bmatrix} \begin{bmatrix} \tilde{\mathbf{q}} \\ \mathbf{Q} \end{bmatrix} + i\omega \begin{bmatrix} \mathbf{0} & \mathbf{0} \\ \mathbf{0} & \mathbf{R} \end{bmatrix} \begin{bmatrix} \tilde{\mathbf{q}} \\ \mathbf{Q} \end{bmatrix} + \\ &\begin{bmatrix} \tilde{\mathbf{\Phi}}^T\left(\mathbf{K}_u + \mathbf{C}_{uV}\mathbf{K}_V^{-1}\mathbf{C}_{uV}^T\right)\tilde{\mathbf{\Phi}} & \tilde{\mathbf{\Phi}}^T\mathbf{C}_{uV}\mathbf{K}_V^{-1} \\ \mathbf{K}_V^{-1}\mathbf{C}_{uV}^T\tilde{\mathbf{\Phi}} & \mathbf{K}_V^{-1} \end{bmatrix} \begin{bmatrix} \tilde{\mathbf{q}} \\ \mathbf{Q} \end{bmatrix} = \begin{bmatrix} \tilde{\mathbf{\Phi}}^T\mathbf{F} \\ \mathbf{0} \end{bmatrix} \end{aligned} \quad (21)$$

Remarks:

- This method requires the knowledge of the optimal values of the electric inductances before the computation of the eigenmodes.

- The change of variables from physical coordinates $\mathbf{U}$ to modal coordinates $\mathbf{q}$ and the modal truncation concern only the mechanical displacement and not the electrical unknown field $\mathbf{Q}$. This is justified by the fact that it is unnecessary to reduce $\mathbf{Q}$ since its size is small and represents the number of piezoelectric patches.

- Substituting $\tilde{\mathbf{\Phi}}_{qi}$ in terms of $\tilde{\mathbf{\Phi}}_{si}$ from the second line of Eq. (19), the modal problem amounts to solve:

$$\left(-\tilde{\omega}_i^2\mathbf{M}_u + \left[\mathbf{K}_u + \mathbf{C}_{uV}\mathbf{K}_V^{-1}\mathbf{C}_{uV}^T - \mathbf{C}_{uV}\mathbf{K}_V^{-1}\left(\mathbf{K}_V^{-1} - \tilde{\omega}_i^2\mathbf{L}\right)^{-1}\mathbf{K}_V^{-1}\mathbf{C}_{uV}^T\right]\right)\tilde{\mathbf{\Phi}}_{si} = \mathbf{0} \tag{22}$$

  Two cases can be distinguished, depending on the value of the inductance:

  - short-circuit case (inductances $L^{(i)} = \mathbf{0}$)

$$\left[\mathbf{K}_u - \tilde{\omega}_i^2\mathbf{M}_u\right]\tilde{\mathbf{\Phi}}_{si} = \mathbf{0} \tag{23}$$

  - open-circuit case (inductances $L^{(i)} = \infty$)

$$\left[\left(\mathbf{K}_u + \mathbf{C}_{uV}\mathbf{K}_V^{-1}\mathbf{C}_{uV}^T\right) - \tilde{\omega}_i^2\mathbf{M}_u\right]\tilde{\mathbf{\Phi}}_{si} = \mathbf{0} \tag{24}$$

4. Resolution and quasi-static correction

Whatever the projection base, the found system of differential equations can be solved by Duhamel integral or by step-by-step integration methods (for example, Newmark, Wilson). Once the system is numerically solved, the modal amplitudes are introduced in Eq. (7) (or depending on the case Eq.(13); (17); (20)) to give the structural response in terms of displacement.

In the transformation of the physical equations to the reduced set of modal equations, the choice of the number of modes to retain is typically driven by the need to span the frequency content of interest. That is, the frequency of the highest mode retained should sufficiently exceed the frequency content of the applied time history loading by a predetermined margin. However, this criterion only addresses the frequency depending portion of the applied load $f(\omega)$ and ignores the spatial portion $\mathbf{F}_0$. Undesirable inaccuracies in the response calculations can occur by not considering the effects of modal truncation on the spatial portion of the applied load. Obviously, a reduction in the spatial load truncation can be realized by increasing the number of retained modes. However, when we significantly increase the number of modes retained in the projection base in order to converge to an "accurate"

solution, the size of the system and therefore the computational cost also increases, which leads to the loss of the advantages of the modal truncation method. There are techniques that not only address the problem of spatial load truncation, but also improve the modal efficiency with which the solution converges. The mode acceleration method and modal truncation augmentation method are two such method [18, 19].

The modal truncation augmentation method attempts to correct for the inadequate representation of the spatial loads in the modal domain by creating additional "pseudo eigenvector" or "quasi-static correction" to include in the modal set for the response analysis. A "pseudo eigenvector", $\mathbf{X}$, is determined by solving the following equation:

$$\mathbf{K}_u \mathbf{X} = \mathbf{F}_0 \tag{25}$$

This "pseudo eigenvector" $\mathbf{X}$ is not orthogonal with respect to the mass matrix of the problem. Thus, a modified Gram-Schmidt algorithm is applied to orthogonalize this eigenvector and build an orthogonal basis $\bar{\mathbf{\Phi}}$. In the short-circuited case, this algorithm can be defined as follows [20]

$$\bar{\mathbf{X}} = \mathbf{X} - \sum_{i=1}^{M_s} (\mathbf{\Phi}_i^T \mathbf{M}_u \mathbf{X}) \mathbf{\Phi}_i \tag{26}$$

$$\mathbf{\Phi}_s = \bar{\mathbf{X}} / (\bar{\mathbf{X}}^T \mathbf{M}_u \bar{\mathbf{X}})^{(1/2)} \tag{27}$$

where $\bar{\mathbf{X}}$ is an auxiliary vector and $\mathbf{\Phi}_s$ is the orthonormalized pseudo eigenvector.

The vector $\mathbf{\Phi}_s$ is appended to the retained modal set, $\mathbf{\Phi}$ for the case of projection on the short-circuited basis, to construct the pseudo modal set, $\bar{\mathbf{\Phi}}$

$$\mathbf{\Phi} \mapsto \bar{\mathbf{\Phi}} = [\mathbf{\Phi}\ \mathbf{\Phi}_s] \tag{28}$$

5. Numerical examples and experimental validation

5.1. Experimental validation of the proposed FE formulation

In this first example, we propose to validate the proposed FE element formulation and piezoelectric assumptions by comparison to experimental results. The system under study consists of a cantilever beam, already used

in [12], partially covered with two collocated piezoelectric elements polarized in opposite directions (Figure 2). The beam material is elastic, homogeneous and isotropic, of density ρ_b and Young's modulus Y_b. The piezoelectric material constants are its density ρ_p, Young's modulus Y_p, coupling piezoelectric constant $\bar{e}_{31}$ and dielectric constant $\bar{\epsilon}_{33}$. The system geometry is defined by the length/thickness of the beam and the piezoelectric patches, respectively denoted l_b/h_b and l_p/h_p; b denotes their common width. Finally, the piezoelectric patches limits are defined by x_- and x_+, with $x_+ - x_- = l_p$. All geometrical and mechanical data of the studied system are given in Table 1 and Figure 2.

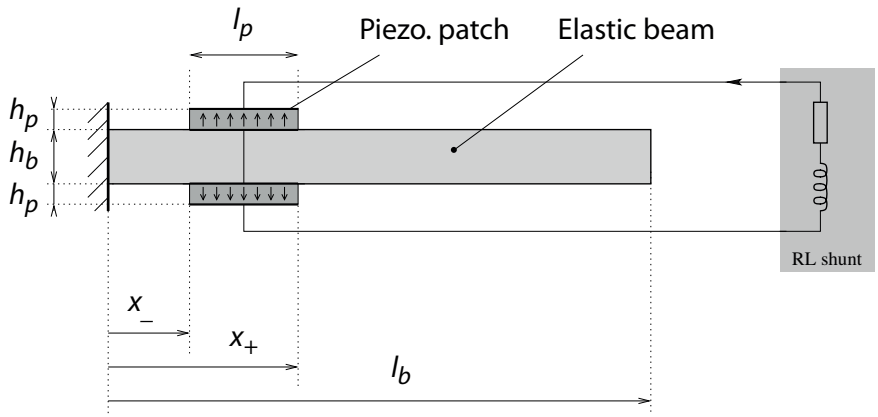

Figure 2: Beam with two piezoelectric patches.

Concerning the experimental setup (Figure 3), the beam is clamped with a vice. An non-contact electromagnetic driving system is used, composed of a small magnet glued on the structure with bees-wax, subjected to the magnetic field created by a coil, fed by a sine electrical signal. The force acting on the beam is estimated by measuring the current intensity in the coil, proportional to the force. The beam motion is obtained with a laser Doppler vibrometer, that measures the velocity of the beam in one point.

For the finite element model, the beam is modeled in 1D using 41 beam elements with three degrees of freedom per node (axial and transverse displacements and the rotation). The portion of the beam covered by the piezoelectric patches is modeled according to laminated theory [17].

Parameters	Beam	Values	Piezo.	Values
Lengths [mm]	l_b	170	l_p	25
Thicknesses [mm]	h_b	2	h_p	0.5
Width [mm]	b	20	b	20
Patches position [mm]			x_-	0.5
Densities [kg/m^3]	ρ_b	2800	ρ_p	8500
Young's moduli [GPa]	Y_b	72	Y_p	66.7
Piezoelectric constant [C/m^2]			$\bar{e}_{31}$	-14
Dielectric constant [F/m]			$\bar{\epsilon}_{33}$	$2068\epsilon_0$

Table 1: Numerical values of system parameters. $\epsilon_0 = 8.854 \cdot 10^{-12}$ F/m is the free space permittivity.

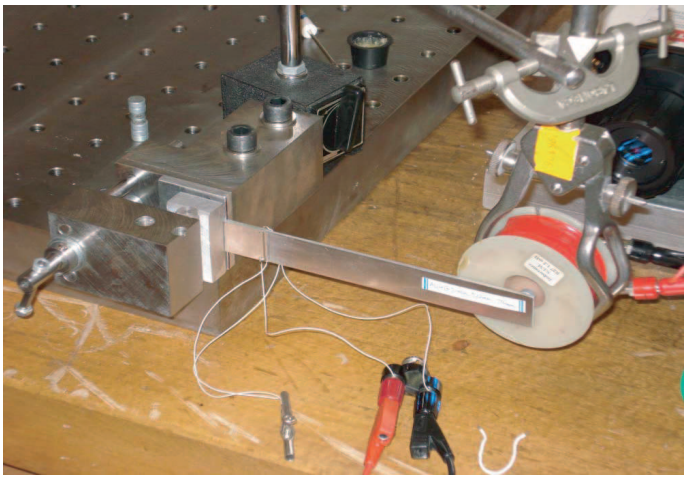

Figure 3: Experimental setup.

Table 2 presents the first fourth experimental and numerical eigenfrequencies of the beam (with short-circuit or open-circuit patches) and the corresponding effective electromechanical modal coupling factor (EEMCF), characterizing the energy exchanges between the elastic structure and the piezoelectric patches and defined by:

$$k^2_{eff,i} = \frac{\hat{\omega}^2_{si} - \omega^2_{si}}{\omega^2_{si}} \tag{29}$$

The first, second and fourth frequencies are associated to the first three bending modes lower than 1000 Hz, while the third one corresponds to the

	Short circuit freq. [Hz]			Open circuit freq. [Hz]			Coupling factors	
Modes	f_i FE	f_i Exp.	Error %	$\hat{f}_i$ FE	$\hat{f}_i$ Exp.	Error %	$k_{\text{eff},i}$ FE	$k_{\text{eff},i}$ Exp.
1 flex. (F)	48.96	51.64	5.20	49.42	52.17	5.27	0.137	0.144
2 flex. (F)	337.1	337.0	0.03	340.7	340.2	0.15	0.145	0.138
1 tors. (T)	–	853.0	–	–	854.0	–	–	0.050
3 flex. (F)	951.8	936.3	1.65	960.6	940.0	2.20	0.137	0.089

F: Bending mode, T: Torsional mode

Table 2: Natural frequencies and coupling coefficients, from finite element computation (FE) and experiments (Exp.).

first torsional vibration mode. This classification was found from the shapes of these modes, which are not shown here for the sake of brevity. Moreover, as expected for bending modes, the natural frequencies of the open-circuit modes are higher than those obtained in the short-circuited case due to the electrical effect of the patch. One can remark that the torsional mode has a low coupling coefficient as compared to the ones of the flexural modes. It would be zero in theory, since the extensional motion of the piezoelectric patches are not activated when the beam undergoes torsion. Moreover, since the FE model does not include torsion d.o.f., no FE values are available in Table 2. Another remark is that for the first mode, the measured value of the effective coupling coefficient $k_{\text{eff},i}$ is higher that the finite-elements one. One would expect the opposite, for example because of non-perfect bonding, as found for the second and third flexural modes. A difference between model and experiments is the wrapped electrode, that is used to easily solder the electric wire to the lower electrode, on the piezoelectric patch upper face. It locally modifies the electric field intensity and direction near the edge of the piezoelectric patch. This may explain the observed increase of coupling coefficient in the experiments, even if the exact effect of the wrapped electrode is difficult to characterize without a three dimensional electromechanical simulation. This is beyond the scope of the present article.

The vibratory response of the system subjected to a harmonic force applied to the tip of the beam is evaluated experimentally and by the proposed reduced order FE formulation. The short-circuited basis with the first 12 modes is used. In order to achieve maximum vibration dissipation of the

second mode, the patch is tuned to an RL shunt circuit. The resistance R and the inductance L can be adjusted and properly chosen to maximize the damping effect of a particular mode. The optimal resistance and inductance of the ith mode for a series resonant shunt are given by [3]:

$$R^{\text{opt}} = \frac{\sqrt{2k_{\text{eff},i}^2}}{C\omega_i(1+k_{\text{eff},i}^2)} \tag{30a}$$

$$L^{\text{opt}} = \frac{1}{C\omega_i^2(1+k_{\text{eff},i}^2)} \tag{30b}$$

where ω_i is the short circuit natural frequency of the ith mode, C is the capacitance of the piezoelectric patch and $k_{\text{eff},i}$ is the effective electromechanical coupling coefficient given in Eq. (29). The taken values of the resistance and of the inductance for the selected mode are: $R = 7900\ \Omega$ and $L = 21.8\ H$.

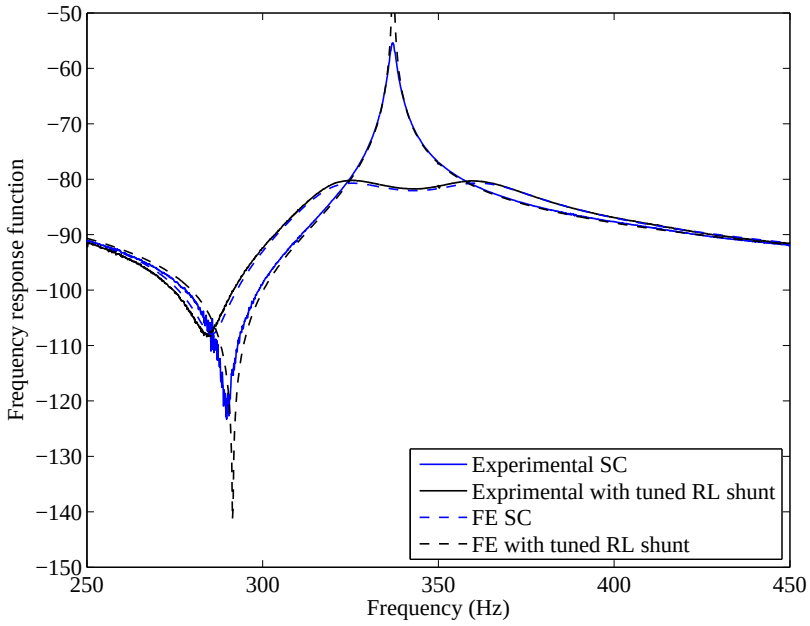

Figure 4: Beam tip frequency response functions. '—': experimental; '- -': finite element.

Figure 4 shows the frequency response function with and without shunt damping at the tip of the beam, computed from the proposed FE formula-

tion as well as from the experiments. An excellent agreement is obtained between simulations and experiments. The main difference lies in the structural damping that is not taken into account in the FE model, which leads to infinite responses, in short circuit, at the beam resonances. In the experiments, an attenuation of 25dB is obtained with the shunt damping as compared with the short-circuit resonance.

5.2. Comparison of model reduction methods for cantilever beam with shunted piezoelectric patch

In this example, we propose to compare the proposed modal reduction techniques in terms of prediction of vibration attenuation with piezoelectric shunt on a simple system. The system under study consists of a cantilever beam with one piezoelectric device, as sketched in Figure 5. The beam is

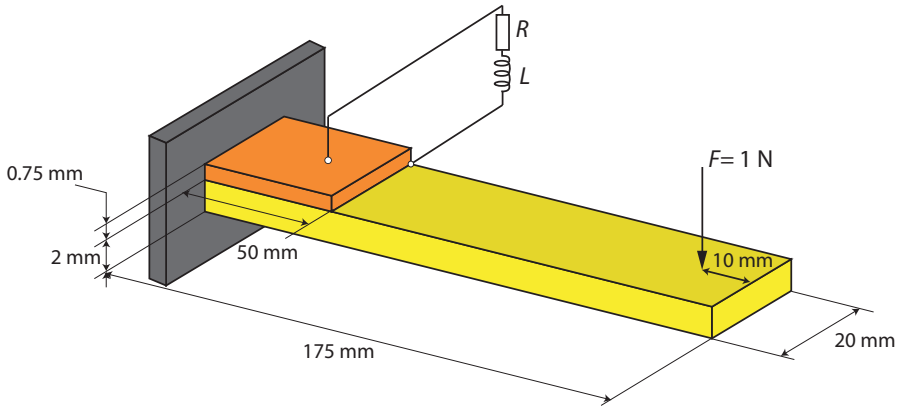

Figure 5: Cantilever beam partially covered with collocated piezoelectric element: geometrical data.

made of aluminum (E = 74 GPa, ν = 0.33, and ρ = 2700 kg/m^3) with L_b=175 mm (length), w_b=20 mm (width), and h_b=2 mm (thickness). The piezoelectric element in PIC-151 is assumed to be perfectly bounded to the beam and has the same width. For the mechanical and electrical characteristics of the piezoelectric material PIC-151, the reader can be referred to [16]. Concerning the finite element discretization, the beam is modeled in 2D using 672 four nodes plate elements (QUAD4). The portion of the plate covered by the piezoelectric patch and the patch itself is modeled according to laminated theory.

Table 3 presents the first five eigenfrequencies of the beam (with short-circuit or open-circuit patches) and the corresponding effective electromechanical modal coupling factor (EEMCF).

The first, second and fourth frequencies are associated to the first three bending modes lower than 1100 Hz, while the third one corresponds to the first bending mode in the plane and the fifth frequency corresponds to the first torsional vibration mode.

Type	Short circuit frequencies	Open circuit frequencies	k_{eff}
F	71.89	73.48	21.15
F	379.49	383.97	15.42
F_p	587.02	587.02	0
F	969.11	970.05	4.41
T	1048.71	1048.71	0

F: Bending mode, F_p Bending mode in the plane, T: Torsional mode

Table 3: Computed frequencies (Hz) of the beam and the electromechanical coupling coefficient.

The beam is now excited by a harmonic transverse load (see Figure 5). In addition, no mechanical damping was introduced in this example. The vibration output is detected at the excitation point. In order to achieve maximum vibration dissipation of the first mode, the patch is tuned to an RL shunt circuit.

Figure 6 presents the frequency response of the system, with and without shunted patch, in terms of the transverse displacement computed with a direct method in which the displacement and the charge vectors are calculated at each frequency step. We can see the effect of the shunt in the vibration damping of the selected mode.

Figures 7 and 8 show a comparison between the frequency responses of the cantilever beam when the shunt circuit is tuned to damp the first vibration mode. We compare all the proposed reduction techniques to the direct approach. We can deduce that:

- The reduced order models built from the short-circuit and the open circuit bases converge with a large number of eigenvectors. With a

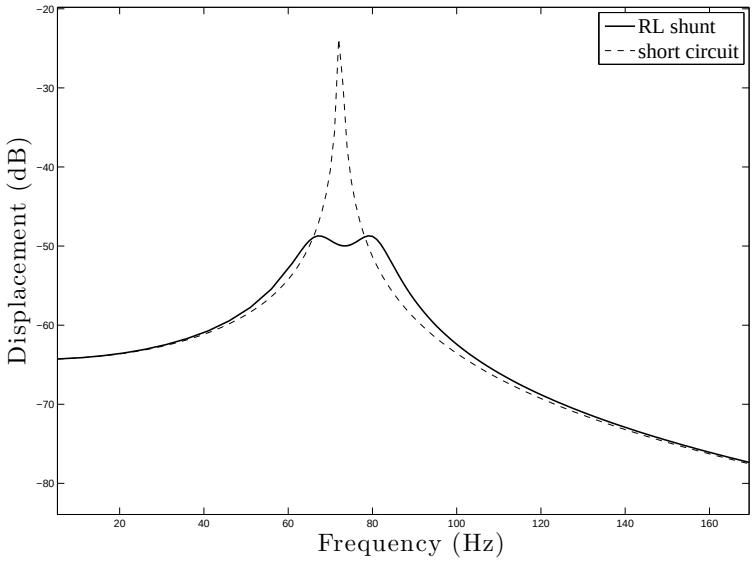

Figure 6: Frequency response function of the cantilever beam with and without patch and subjected to a harmonic transverse load.

small number of eigenvectors, the short-circuit basis overestimates the attenuation while the open-circuit basis underestimates it.

- The reduced order model computed from the combined basis gives excellent results with only one short-circuited mode and one open-circuited mode. This efficiency is related to the introduction of additional electromechanical coupling terms in the reduced system, which allows better modeling of the effects of the piezo-patches and the shunt-circuit on the response of the system.

- The reduced order model built from the coupled basis is extremely effective. The model response converges when projecting the unknown mechanical displacements only on the first two eigenvectors. The attenuation of a resonance mode with the shunt technique is characterized by a decrease of the amplitude of the peak around the targeted frequency. Two peaks with very low amplitude, around the frequency to attenuate, appear in the damped response. In this example, these two peaks correspond to the first two modes of the coupled basis with mode

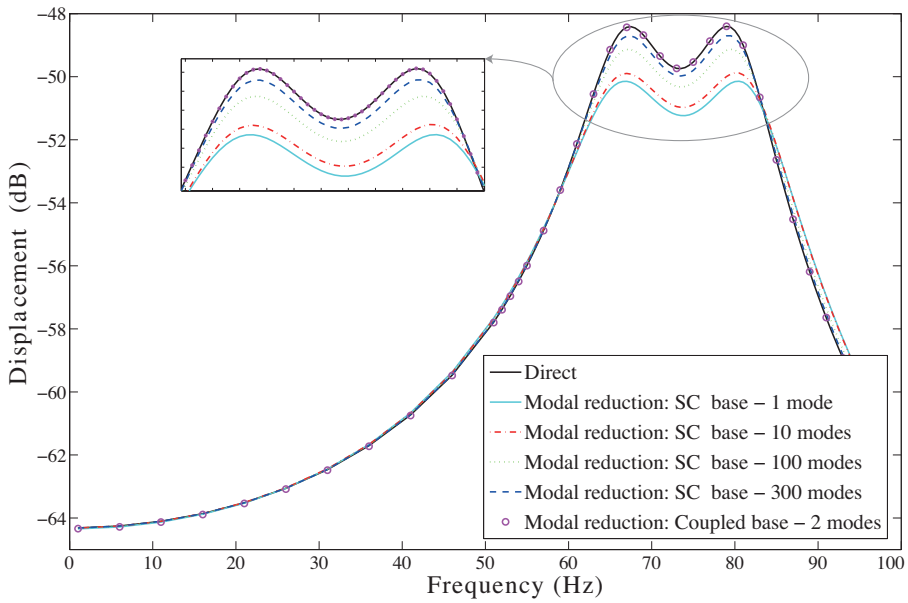

Figure 7: Frequency responses of the cantilever beam with shunted piezoelectric patch: comparison between (i) the direct approach, (ii) modal reduction using short-circuited basis and (iii) modal reduction using coupled basis.

shapes very close. This leads us to conclude that this basis formed by the real modes of the coupled system (elastic structure with shunted piezoelectric patches), is very effective in the prediction of vibration attenuation.

5.3. Multimode shunt control of a vibrating plate

In this third example, a clamped rectangular plate with two rectangular piezoelectric patches perfectly bonded on its surface is considered. The plate of 2-mm-thick is made in aluminum and the patches of 0.5-mm-thick are in PIC 151 (we used the same properties as the previous example). The geometrical data of the problem are given in Figure 9. Concerning the finite element discretization, the plate is modeled with 600 QUAD4. The portion of the plate covered by the piezoelectric patches and the patch itself are modeled according to the laminated theory. In this theory, the composite plate model, with piezoelectric layers polarized along the thickness, combines an equivalent single-layer approach for the mechanical behavior with a layer-wise representation of the electric potential in the thickness direction (see

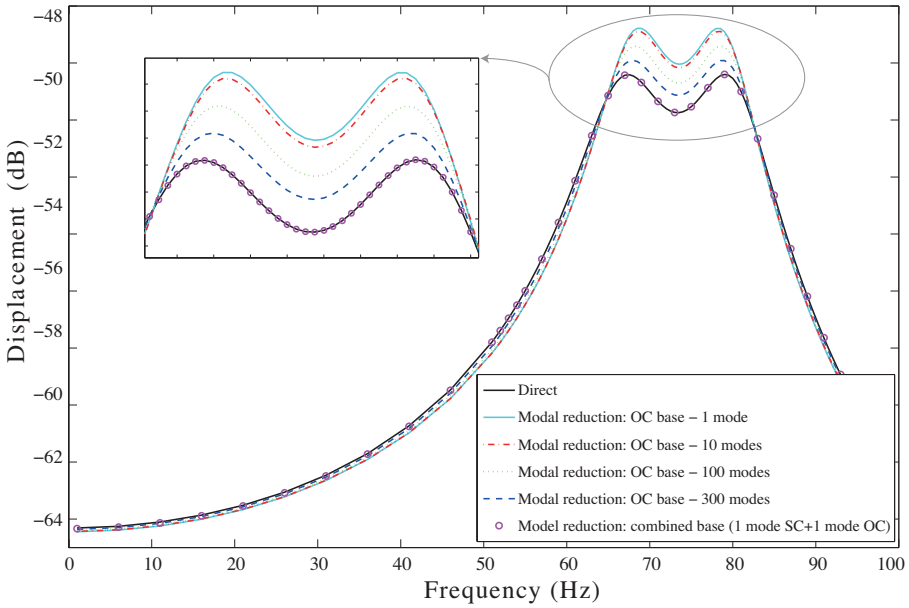

Figure 8: Frequency responses of the cantilever beam with shunted piezoelectric patch: comparison between (i) the direct approach, (ii) modal reduction using open-circuited basis and (iii) modal reduction using combined basis.

[15] for more details about this formulation). The plate is excited by a normal unit sinusoidal force as sketched in Figure 9. The vibration output is detected at the excitation point, where the displacement reaches a maximum. In addition, mechanical damping was introduced through a modal damping coefficient $\xi = 0.001$ for all eigenmodes in the selected reduced modal basis.

Table 4 presents the first ten eigenfrequencies of (i) the clamped plate with all patches short-circuited, (ii) the clamped plate with all patches open-circuited and (iii) the coupled problem given by Eq. (19). For the third case, the two patches are tuned to the first two vibration modes respectively and the used optimal inductances are computed from Eq. (30b) : L_1 =6.95 H and L_2 =3.75 H (for the resistances of the shunt circuit, we used Eq. (30a): R_1 =214 Ω and R_2 =544 Ω). For each frequency of the open-circuit case, except for modes without electromechanical coupling, corresponds two frequencies in the coupled case (one lower and the other higher to this frequency). The mode shapes associated to these frequencies are very similar to the mode of the open-circuited original one. These modes are not shown here for the sake of brevity.

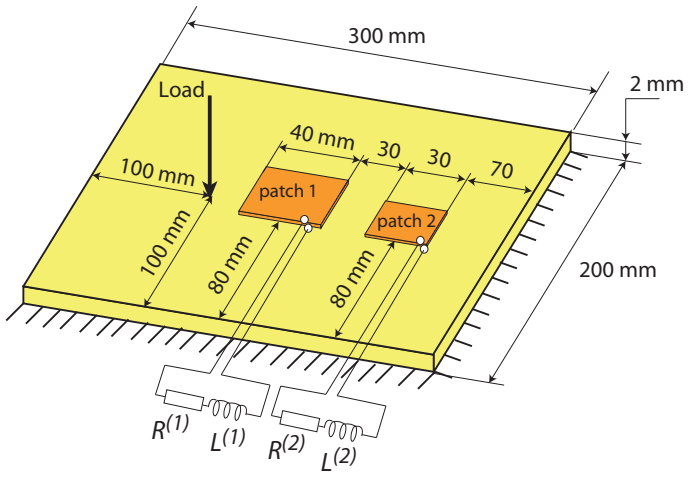

Figure 9: Clamped plate partially covered with two collocated piezoelectric elements: geometrical data.

Short circuit frequencies	Open circuit frequencies	Coupled frequencies
326.98	327.85	306.68
512.76	516.10	348.79
824.66	827.05	486.10
829.68	829.68	544.23
1005.77	1005.77	829.68
1265.51	1265.61	836.79
1291.48	1291.48	1005.77
1600.37	1604.25	1265.63
1727.30	1727.30	1291.48
1751.45	1763.06	1617.75

Table 4: Computed frequencies (Hz) of the plate with piezoelectric patches in: (i) short-circuit case, (ii) open-circuited case and (iii) coupled case.

As mentioned previously, the resonant shunts are tuned respectively to the first and second mode in order to achieve maximum energy dissipation of these modes. Figure 10 presents the frequency response of the system in terms of the transverse displacement computed with direct nodal method. This figure shows that the resonant magnitude of the selected modes has been significantly reduced. In fact, the strain energy contained in the piezoelectric

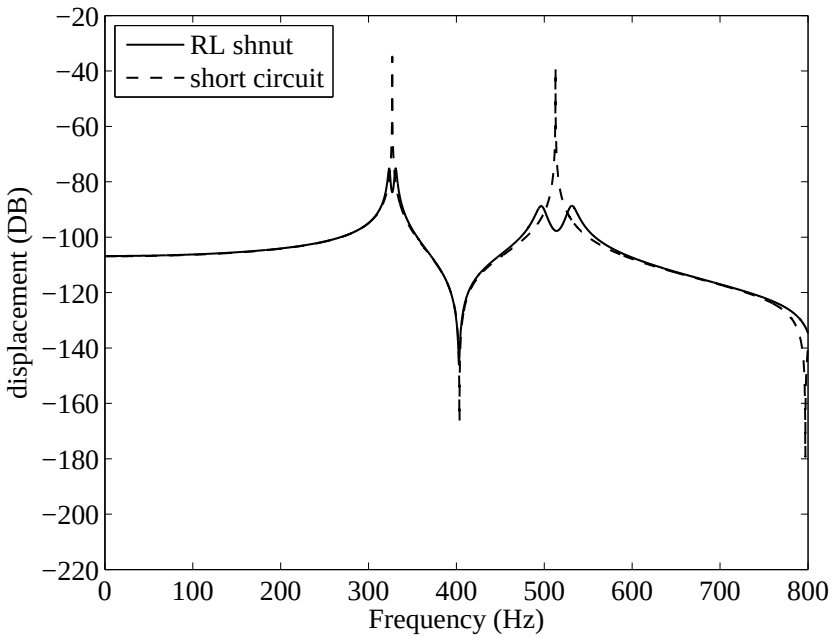

Figure 10: Frequency response function of the plate subjected to a harmonic load with and without shunted piezoelectric patches.

material is converted into electrical energy and hence dissipated into heat using the RL shunt devices.

Figures 11 and 12 show a comparison of the frequency response of the shunted system computed with direct method to those computed with modal reduction method using the different proposed bases. A static correction is appended to all the retained modal bases. These results are consistent with those obtained from the previous example:

- The reduced order models built from the short-circuited or open-circuited bases does not fully converge with a reduced number of eigenvectors.
- Using the combined bases, excellent results are obtained in the resonance zones when the unknown mechanical displacements are projected on the basis formed by the first two short-circuited modes and the first two open-circuited. Using the first 38 short-circuited (respectively open-circuited) modes and the first two open-circuited (respectively short-circuited) modes, the response of the model converges in areas of

resonance and also outside these areas.

- The reduced order model built from the coupled basis gives excellent results compared to the results of the direct method. This convergence is achieved by using the first 40 modes. We note that with only four modes (modes resulting from the resonant shunt technique), the convergence is limited to resonant frequencies and is not assured in the other areas.

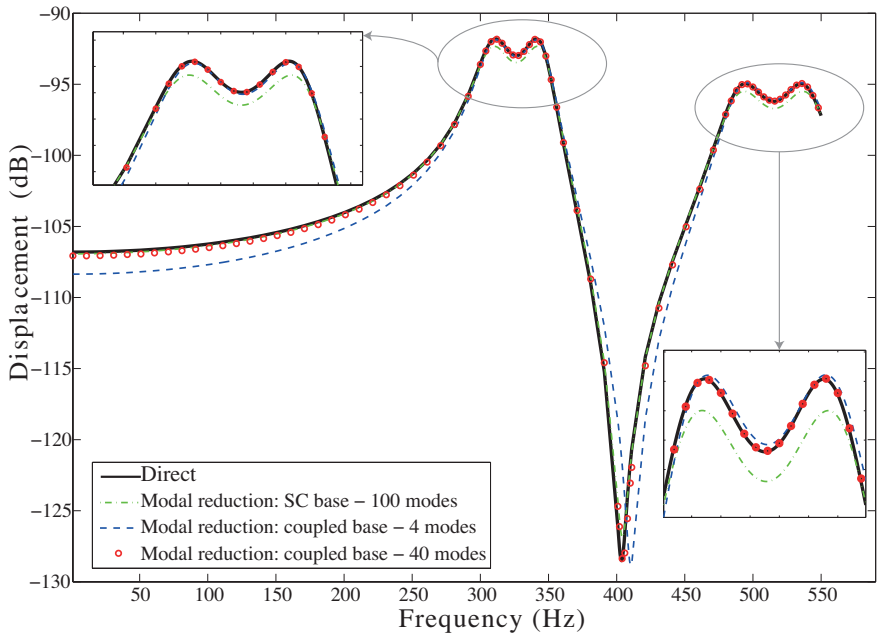

Figure 11: Frequency responses of the plate with shunted piezoelectric patches: comparison between (i) the direct approach, (ii) modal reduction using short-circuited basis and (iii) modal reduction using coupled basis.

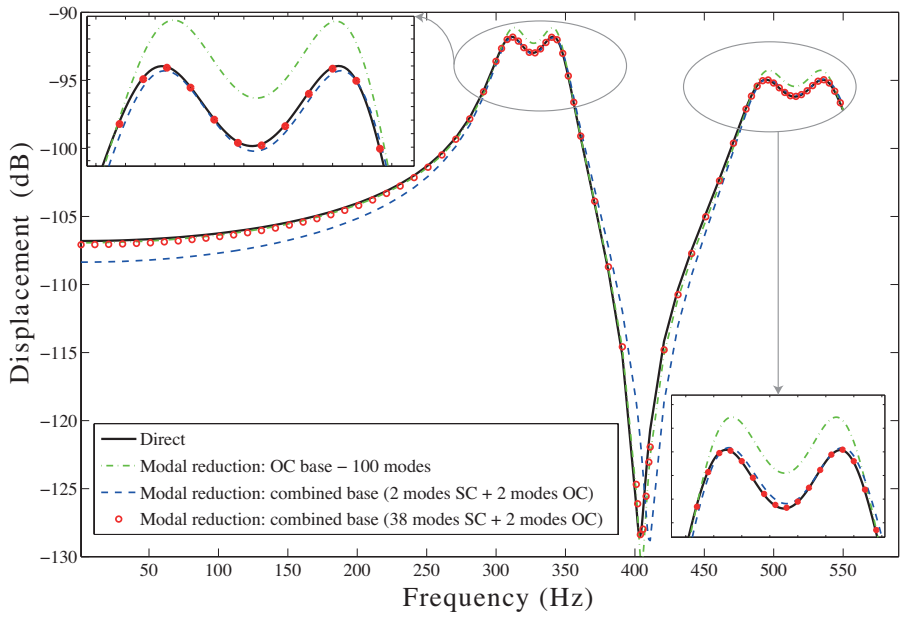

Figure 12: Frequency responses of the plate with shunted piezoelectric patches: comparison between (i) the direct approach, (ii) modal reduction using open-circuited basis and (iii) modal reduction using combined basis.

From these examples, we can deduce the good performances of the original coupled and combined bases to predict damping of elastic structures using shunted piezoelectric patches. Compared to classical short-circuit and open-circuit bases, these bases provide good convergence with a small number of modes. However, they present some inconveniences and limitations:

- The coupled basis can be used only for a resonant shunt and requires knowledge of the optimal values of inductances before the modal projection.
- The combined basis requires two modal calculations to find short-circuit and open-circuit modes. The resulting basis is not orthogonal with respect to the mass and stiffness matrices. The modified Gram-Schmidt orthogonalization process can be applied in order to orthogonalize this basis.

6. Conclusions

In this paper, reduced order finite element formulations for passive reduction of structural vibration by means of shunted piezoelectric system are presented. Two new reduced-order models, based on a normal mode expansion, are developed: (i) the combined basis, and (ii) the coupled basis. Despite their reduced size, these model are proved to be very efficient with a reduced number of modes compared to classical bases for simulations of vibration attenuation of selected frequency resonances. However, some drawbacks remain and concern the necessity of two modal calculations for the combined basis and the knowledge of the optimal values of inductors before projection for the coupled basis. Despite these disadvantages, these new techniques can be recommended for the resolution of electromechanical problems with shunt devices.

References

[1] M.A Trindade, A. Benjeddou, R. Ohayon, Finite element modeling of hybrid active-passive vibration damping of multilayer piezoelectric sandwich beams. Part 1: formulation, *International Journal for Numerical Methods in Engineering*, **51(7)**, 835–854, 2001.

[2] B. Kim, G.N. Washington, H.-S. Yoon, Active Vibration Suppression of a 1D Piezoelectric Bimorph Structure Using Model Predictive Sliding Mode Control, *Smart Structures and Systems*, **11(6)**, 623–635, 2013.

[3] N.W. Hagood, A.V. Flotow, Damping of structural vibrations with piezoelectric materials and passive electrical networks, *Journal of Sound and Vibration*, **146(2)**, 243–268, 1991.

[4] F. dellIsola, C. Maurini, M.A. Porfiri, Passive damping of beam vibrations through distributed electric networks and piezoelectric transducers: prototype design and experimental validation, *Smart Materials and Structure*, **13(2)**, 299-308, 2004.

[5] M. Collet, K.A. Cunefare, M.N. Ichchou, Wave motion optimization in periodically distributed shunted piezocomposite beam structures, *Journal of Intelligent Material Systems and Structures*, **20(7)**, 787–808, 2009.

[6] F. Casadei, M. Ruzzene,L. Dozio, K.A. Cunefare, Broad band vibration control through periodic arrays of resonant shunts: experimental investigation on plates, *Smart Materials and Structures*, **19(1)**, 015002, 2010.

[7] A. Belloli, D. Niedereberger, S. Pietrzko, M. Morari, P. Ermanni, Structural vibration control via rl-shunted active fiber composites, *Journal of Intelligent Material Systems and Structures*, **18(3)**, 275–287, 2007.

[8] D. Niederberger, A. Fleming, S.O.R. Moheimani, M. Morari, Adaptive multi-mode resonant piezoelectric shunt damping, *Smart Materials and Structures*, **13(5)**, 1025–1035, 2004.

[9] D. Guyomar, A. Faiz, L. Petit, C. Richard, Wave reflection and transmission reduction using piezoelectric semipassive nonlinear technique, *The Journal of the Acoustical Society of America*, **119(1)**, 285–298, 2006.

[10] J. Ducarne, O. Thomas, J.-F. Deü, Structural vibration reduction by switch shunting of piezoelectric elements: modeling and optimization, *Journal of Intelligent Materials Systems and Structures*, **21(8)**, 797–816, 2010.

[11] W. Larbi, J.-F. Deü, M. Ciminello, R. Ohayon, Structural-acoustic vibration reduction using switched shunt piezoelectric patches: a finite element analysis, *Journal of Vibration and Acoustics*, **132(5)**, 051006, 2010.

[12] O. Thomas, J.-F. Deü, J. Ducarne, Vibrations of an elastic structure with shunted piezoelectric patches: efficient finite elements formulation and electromechanical couplings coefficients. *International Journal for Numerical Methods in Engineering* **80(2)**, 235–268, 2009.

[13] J.-F. Deü, W. Larbi, R. Ohayon, R. Sampaio, Piezoelectric shunt vibration damping of structural-acoustic systems: Finite element formulation and Reduced-Order Model, *Journal of Vibration and Acoustics*, **136(3)**, 031007, 2014.

[14] W. Larbi, J.-F. Deü, R. Ohayon, R. Sampaio, Coupled FEM/BEM for control of noise radiation and sound transmission using piezoelectric shunt damping, *Applied Acoustics*, **86**, 146–153, 2014.

[15] W. Larbi, J.-F. Deü, R. Ohayon, Finite element formulation of smart piezoelectric composite plates coupled with acoustic fluid, *Composite Structures*, **94(2)**, 501-509, 2012.

[16] L. Pereira da Silva, W. Larbi, J.-F. Deü, Topology optimization of shunted piezoelectric elements for structural vibration reduction, *Journal of Intelligent Material Systems and Structures*, **26(10)**, 1219-1235, 2015.

[17] J. Reddy, *Mechanics of Laminated Composite Plates and Shells: Theory and Analysis*, CRC, Boca Raton, FL, 2004.

[18] J.M. Dickens, J.M. Nakagawa, M.J. Wittbrodt, A critique of mode acceleration and modal truncation augmentation methods for modal response analysis, *Computers & Structures*, **62(6)**, 985–998, 1997.

[19] H.L. Soriano, F.Venâncio Filho, On the modal acceleration method in structural dynamics. Mode truncation and static correction, *Computers & Structures*, **29(5)**, 777–782, 1988.

[20] L. Meirovitch, *Computational Methods in Structural Dynamics*, Springer Netherlands, 1980.